2021-24-0018 Published 05 Sep 2021

In-Cylinder Heat Transfer Determination Using Impulse Response Method with a Two-Dimensional Characterization of the Eroding Surface Thermocouple

Carl Caruana, Mario Farrugia, and Pierluigi Mollicone Univ of Malta

Emiliano Pipitone Univ of Palermo

Gilbert Sammut Dolphin N2 Ltd

Citation: Caruana, C., Farrugia, M., Mollicone, P., Pipitone, E. et al., "In-Cylinder Heat Transfer Determination Using Impulse Response Method with a Two-Dimensional Characterization of the Eroding Surface Thermocouple," SAE Technical Paper 2021-24-0018, 2021, doi:10.4271/2021-24-0018.

Abstract

Heat transfer from the cylinder of internal combustion engines has been studied for decades, both in motored and fired configurations. Its understanding remains fundamental to the optimization of engine structures and sub-systems due to its direct effect on reliability, thermal efficiency and gaseous emissions. Experimental measurements are usually conducted using fast response surface thermometers, which give the instantaneous cylinder surface temperature. The transient component of heat flux through the cylinder wall was traditionally obtained from a spectral analysis of the surface temperature fluctuation, whereas the steady-state component was obtained from Fourier's law of conduction. This computation inherently assumes that heat flows in one-dimension, perpendicular to the heated surface in a semi-infinite solid with constant thermo-physical properties. Results from this computation are prone to significant uncertainties originating from numerous sources, most of which related to the limitations in the technology of surface thermometry and the method used to convert the surface temperature to heat flux. In this study, a single cylinder version of a 2.0 liter engine operating in the pressurized motored configuration was instrumented at two locations in the cylinder head with surface thermocouples of the eroding type, one fitted along the cylinder central axis and another in the squish region. Three different eroding surface thermocouples were tested on the experimental setup, at the same location. Results from this research showed that heat flux through the surface thermocouple is at least two-dimensional. This paper presents a detailed account of the uncertainties in the determined heat flux, expected from the use of surface thermocouples. The paper also presents an application of a method by which the surface temperature can be converted to heat flux, accounting for multi-dimensional effects. This method is known as the 'Impulse Response', and was coupled to a two-dimensional finite element model of the surface thermocouple.

Introduction

The heat transferred from the cylinder of an internal combustion engine is a research area that had been active for several decades due to its direct effect on engine performance and durability. Few methods have been proposed by which the instantaneous heat transfer from the cylinder can be obtained; some of which involve a direct measurement using fast-response surface thermometers, whereas others utilize less intrusive methods like the CARS measurement method, or an indirect determination using sub-surface thermocouples. The method which seems to remain popular is that of surface thermocouples. Despite its popularity, this method does not come without disadvantages. Great care has to be exercised during engine setup, during testing, and also during data processing, for heat flux to be determined with reasonable accuracy.

This research paper will first highlight the sources of inaccuracies that needs to be tackled when performing a heat flux measurement using surface thermocouples, and where possible potential solutions to the mentioned inaccuracies are presented. The second section of the paper will highlight a brief description of the experimental apparatus that was prepared for in-cylinder heat flux research at University of Malta. Lastly, the "Impulse Response Method" coupled to a two-dimensional finite element model of the thermocouple by which the measured cylinder head surface temperature was converted to heat flux is presented in detail. The Impulse Response method is compared to the commonly used method

of Fourier's spectral analysis through results obtained from engine experiments.

Sources of Uncertainty in Heat Flux Determination

From a review of literature spanning over several decades since the first documented use of fast response thermocouples [1], several sources that give rise to uncertainty in heat flux determination were compiled. These can be grouped into at least seven categories, as follows:

1. Spatial location
2. Fitment of surface thermocouples in engine
3. Multi-dimensional heat flow
4. Thermocouple rise time
5. Repeatability of measurement
6. Computation of the time invariant component of heat flux
7. Effect of contaminants on thermocouple surface

In the following sections, each of the above seven sources will be described in detail according to the review of literature, but also from the experience gathered whilst testing the experimental setup described later.

Spatial Location

One of the significant disadvantages of performing direct measurements is that one thermocouple can only supply information at a specific spatial location. It is known that surface temperature and heat flux are spatially sensitive [2, 3, 4], even on the same component's surface. This means that if a direct measurement method is to be used for global heat transfer estimation, more than one thermocouple has to be fitted such that zones with different gas dynamics/heat flux are captured and taken into consideration. Fitment of more than one surface thermocouple can be practically challenging in production-type engines due to complex coolant jackets and oil passages, especially if the remaining six sources of uncertainty are taken into account. Of the reviewed literature, the majority of the researchers settled for a maximum of five surface thermocouples, with the exception of Hohenberg [5] who fitted seventy-two, and recently, Hennes [3] fitted twenty six. The surface thermocouples used by these two authors were specifically made by the same authors from conventional mineral insulated thermocouples. This gave the possibility of fitting more thermocouples due to the smaller diameter of each thermocouple.

Fitment of Surface Thermocouples in Engines

The fitment of surface thermocouples can be done either in the cylinder head, or in the piston crown. Both of these locations offer fitment challenges, but in general, the cylinder head is usually preferred due to the lesser complication originating from the movement of the piston that would require a grasshopper linkage system, with the associated short lifetime of the thermocouple wires [3]. Despite the lesser complexity of fitment at the cylinder head, one must not underestimate the errors that could potentially arise due to improper fitment of the thermocouple. This source of error can manifest itself in at least two ways. First, if the thermocouple is fitted in a location which is affected by multi-dimensional heat flow, the measured surface temperature and heat flux can be subjected to significant error magnitudes. In a study by Alkidas [6], an error of 20% was found to occur at a certain location in a spark ignition (SI) engine, due to the occurrence of multi-dimensional heat flow. This problem is worsened if the thermocouple itself (or its adapter) passes through the coolant jacket, which results in the thermocouple acting as a fin to heat flux, as mentioned by Farrugia [7] and in [8]. Several authors tried to limit the extent of this error, by designing the thermocouples with an insulated boundary to limit the lateral heat flow. While this can offer a partial solution to the problem, it might induce other uncertainties, due to the disturbance of the isotherms by the thermally insulative material.

Apart from the mentioned issues that originate from multi-dimensional heat flow, another concern related to the fitment of the thermocouple is the design of the adapters and/or coolant/gas sealing solutions that are adopted to fix the thermocouple in the engine components. In some cases, adapters threaded in the combustion chamber surface are utilized. Although not widely reported, threaded adapters could possibly lead to heat flux measurement errors due to gas pressure fluctuation occurring between the threads. Overbye [1] outlined this problem very early, and later Farrugia [7] mentioned the same problem when utilizing surface thermocouples in an extension to the exhaust port of a SI engine. For this reason, thermocouples that could be mounted in place with an interference fit are preferred; however this option is often not employed due to the fact that thermocouple maintenance and/or cleaning could only be done through extensive dismantling of the engine. Other authors utilized adhesive media to fix the thermocouples in place, while ensuring a good seal to avoid gas pressure oscillation in crevices. This sealing solution is often not preferred due to the thermally insulative properties of the common adhesives, when compared to the engine material.

Multi-Dimensional Heat Flow within the Thermocouple

The possible errors arising from multi-dimensional heat flow were identified in the previous section. Reference was made to multi-dimensional heat flow occurring within the length of the thermocouple due to presence of nearby cooling jackets. However, errors due to multi-dimensional heat flow extend further than this. The few commercially available fast response thermocouple designs are all made up of more than one material. This means that the surface temperature measurement and computed heat flux are also affected by multi-dimensional effects arising from the thermocouple construction itself. This has been proven by Gatowski [9], Buttsworth

[10] [11], and Wang [12], through thermocouple characterization experiments and engine testing. The extent of the problem varies according to the different timescales of interest. Buttsworth [10] and Wang [12] also attributes this multi-dimensional heat flow as one of the lead causes for the negative heat flux that is usually observed very early in the expansion stroke for both motored operation [13], as well as fired operation [14]. The problem of multi-dimensional heat flow originating from the different materials making up the thermocouple can be solved, by accounting for it in the method used for the conversion of the instantaneous surface temperature to heat flux. The "Impulse Response Method", put forward by Oldfield [15] for turbine measurements, has the capability of accounting for this multi-dimensional heat flow. It was applied to the internal combustion in-cylinder heat flux problem by Wang [12].

Thermocouple Rise Time

The high rotational speed of the internal combustion engine results in a rapid increase in the gas temperature, and a consequential rapid increase in the combustion chamber surface temperature. Due to this, the surface thermocouple employed for heat flux measurements has to be fast enough to ensure that the surface temperature is not attenuated by the thermal capacity of the thermocouple junction. For this reason, few thermocouple constructions have been put forward that are capable of ensuring very fast response times. The first reported occurrence of such fast response thermocouple is by Bendersky [16]. This fast response thermocouple is composed of a thermocouple material with a wire configuration, and another thermocouple material in a tubular form that wraps around the first. The two dissimilar metals are electrically insulated from each other by an oxide layer. The junction at the surface is created by a thin film deposition technique. This type of thermocouple is usually termed as 'Co-Axial', due to its construction. Another thermocouple design is that of the eroding-type thermocouple. In this thermocouple, the two dissimilar metals are of a ribbon type with a 25 μm thickness, parallel to each other. The two dissimilar metal ribbons are separated from each other by a 5 μm Mica sheet. Two other 5 μm Mica sheets are placed at the other two outer sides of the dissimilar metal ribbons. The sandwich is then pressed into a thin tube by two split-tapered inserts. The thermocouple junction is created by abrading the surface perpendicular to the ribbons. Through the abrasion process, slivers are transported from one thermocouple material to the other, over the central Mica. The thermocouple junction can be renewed, and the exposed surface can be ground flush to the instrumented surface contour to prevent any possible perturbations that can arise from the presence of the thermocouple.

It has been reported that both thermocouple designs have the capability of reaching response times lower than 25 μs [9, 17]. While the thermocouple response time of the co-axial thermocouple is dependent on the thin-film at the surface, the response time of the eroding thermocouple is dependent on the thickness of the junction set up by the abrasion process. Buttsworth [18] reported that the response time varies significantly for eroding thermocouples. He attributed this variation to the human variability in establishing the junction.

To obtain response times shorter than the characteristic time expected in engine heat transfer, one needs to consider also the latency of the thermocouple amplifier and the latency of the data acquisition system. Whilst the delay induced by the data acquisition system is considered minute, that of the amplifier might be significant.

To ensure an appropriate response time and a repeatable measurement from the surface thermocouple, during the experimental tests that were conducted on the motored engine, a method was devised by which the surface thermocouple could be tested quickly. A photography flash light (Meike Mk 300) was used to emit a flash of intense light towards the sensing surface of the thermocouple (dismantled from the engine). The temperature measurement was read from the data acquisition system, and the rise time of the thermocouple could be recorded. This procedure was done prior and after every engine testing session as a health check for the thermocouple. Having a quick method by which the rise time can be obtained was found to be very beneficial, not only to ascertain that the rise time is sufficiently small, but also to verify that the characteristic of the thermocouple measurement did not change throughout the engine test matrix. Some variations before and after the engine test matrix were occasionally observed in the thermocouple response.

Repeatability of Measurement

The repeatability of the surface temperature measurement and ensuing heat flux is dependent on several factors. If it is supposed that the parameters that affect heat flux in repeated experimental tests are well reproduced, any variations in heat flux and surface temperature could be reasonably attributable to the surface thermocouple.

From the experimental tests conducted on the engine in the motored mode using eroding surface thermocouples, repeatability was assessed in two different ways. The first method is that explained above which utilizes flash light tests before and after the engine test session. The second method was more direct to the engine measurement. This entailed running the engine at a "standard condition" of 1400 rpm, 80 bar peak in-cylinder pressure (PCP) before and after the experimental test matrix. The surface temperature and calculated heat flux for the two runs were compared. It was found that both the steady-state value and the time-varying component (swing) of the surface temperature showed good repeatability. The steady-state temperature value was found to vary by no more than 5°*C* between the two tests. The temperature swing varied by no more than 3°*C*. Part of this reported variation is attributable to the reproducibility in the intake gas temperature, which varied up to 6°*C* between the two tests, and hence could have induced a slightly different bulk gas temperature.

The degree of repeatability was found to decrease when the engine was tested at the same setpoint conditions, but with different abrasions for the thermocouple junction. From this observation, it was initially concluded that retaining the same thermocouple junction throughout one test matrix is ideal. Later on however, it transpired that even if the same thermocouple junction is retained for long engine testing times,

variations in the thermocouple characteristics might be visible. In general it was found that when this observation was made, the thermocouple junction had a shorter rise time after the test matrix, compared to the rise time before the test matrix was conducted. This observation was not made for every test matrix, but it did occur more than once. It is thought that at certain conditions that promote high bulk gas temperatures, the thermocouple junction may oxidise.

Computation of the Time-Invariant Component of Heat Flux

The total instantaneous heat flux is computed from a summation of a time-invariant component (steady-state) and a time-varying component (transient). The transient component of heat flux was already discussed briefly, and will be dealt with in more detail in the third section of this paper. The steady-state component of heat flux, is usually obtained through Fourier's law of one dimensional conduction, in which the temperature gradient is computed from the temperature difference between the mean of the surface temperature, and another temperature recessed from the surface, at a location at which no temperature fluctuations are recorded. The recessed thermocouple has to be fitted axially close to the surface thermocouple. This method was used by several authors [2, 4, 7].

While the method of obtaining the steady-state component of heat flux just described seems to be the one which is most favored, it is also known that this method is subject to several inaccuracies. First, the recessed thermocouple has to be located at a distance such that no temperature fluctuations are recorded. The distance between the surface and the recessed location is a function of the thermo-physical properties of the material that exists between the surface and the recessed location (usually the same material as the instrumented surface). For a material with a high thermal diffusivity, the distance between the two thermocouples has to be large. This presents a problem when using Fourier's law of one-dimensional conduction due to the existence of multi-dimensional heat flow. For modern engines with aluminum cylinder heads/cylinder blocks, larger errors are expected due to this source, owing from the high thermal diffusivity of aluminum, which requires recessed depths of about 10 mm.

Another problem associated with the use of the Fourier one-dimensional law of conduction originates from the materials used in the surface thermocouple construction, and the material that exists between the surface thermocouple and the recessed thermocouple. The latter is usually the same material as that of the instrumented component. On the other hand, since the surface thermocouple is composed of different materials, the surface temperature measurement might be biased, and not equal to the undisturbed surface temperature. As a result, the temperature gradient used in Fourier's one dimensional law suffers from the same error magnitude by which the surface temperature is biased.

Another error that is usually of a lesser importance than the previous two originates from the uncertainty of the distance between the surface and the recessed thermocouple. Alkidas [4] and Farrugia [7] utilized X-ray imaging of the surface thermocouple to obtain this measurement.

To avoid errors in the steady-state component of heat flux originating from the prescribed three sources, Hoag [19] and Hennes [3] used a simple method which shifts the transient component of heat flux in the y-axis (heat flux axis), such that at the crank angle at which the bulk gas temperature equals the measured wall temperature, the total instantaneous heat flux is zero. While this method seems logically reasonable, the authors of this paper advise caution in using it. The reason behind this is that based on experiments conducted by several authors, it was found that an angular phase difference exists between the bulk gas temperature, the surface temperature and heat flux. In fact, it was shown by Wendland [13] that at the point when the bulk gas temperature equals the wall temperature, the heat flux was found to have a magnitude other than zero. In classical studies that used a quasi-steady approach to heat flux, utilizing Newton's law of cooling resulted in a coefficient of heat transfer of $\pm\infty$.

Effect of Contaminants on Surface Thermocouple

To harness the advantages of the fast rise times offered by the commercially available surface thermocouples, the experimentalist must ensure that during engine testing, the thermocouple surface remains clear of any contaminants that could possibly deposit. This problem can pose worse effects in fired engines compared to motored engines, due to the soot produced by the combustion. On the other hand, in motored operation, whilst soot might not be present, a thin lubrication film might still deposit on the thermocouple surface due to the reciprocating action of the piston and wall lubrication. A study by Overbye [1] had shown that the soot deposits attenuate the recorded surface temperature swing, lower the measured mean of the surface temperature, and induces a phase lag in the surface temperature when compared to the undisturbed measurement. All these observations were observed and confirmed by this paper's authors through experimental testing.

The above sections gave a comprehensive description of the uncertainties and/or limitations that can be expected when testing for in-cylinder heat flux with the direct measurement method of surface thermocouples. While the measurement of surface temperature and heat flux determination presents itself as a challenging endeavor, a balance can still be struck between reliability, practicality and measurement accuracy. The next section gives a brief overview of the experimental setup that was built at the University of Malta for in-cylinder heat flux testing.

Experimental Setup

The in-cylinder heat flux study was conducted on a single cylinder version of an inline four-cylinder, 2.0 liter engine. The engine specifications are given in Table 1. The conversion of the engine from four cylinders to single cylinder is detailed in [20]. The engine was operated in the pressurised motored

TABLE 1 Engine specifications

Make and Model	Peugeot 306 2.0L HDi
Year of Manufacture	2000
Number of Strokes	4-stroke
Number of Cylinders	4, 3 deactivated, 1 active
Valvetrain	8 Valve, OHC
Static Compression Ratio	18:1
Engine Displacement [cc]	1997
Bore [mm]	85
Stroke [mm]	88
Connecting Rod Length [mm]	145
Intake Valve Diameter [mm]	35.6
Exhaust Valve Diameter [mm]	33.8
Intake Valve Opens (1mm lift)	10 CAD ATDC intake
Intake Valve Closes (1mm lift)	20 CAD ABDC intake
Exhaust Valve Opens (1mm lift)	45 CAD BBDC expansion
Exhaust Valve Closes (1mm lift)	10 CAD BTDC exhaust

configuration, using mixtures of air and argon. The pressurised motored method involves motoring the engine with an electric motor, whilst pressurizing its intake (conventionally with air). Intake air pressures up to 2.5 bar can reach fired-like peak in-cylinder pressures of up to 140 bar, depending on the compression ratio and the intake manifold pressure. To recycle the exhausted air, a shunt pipe was introduced between the intake and exhaust manifolds, which recirculated the exhaust back to the intake manifold.

The conventional pressurised motored method was used in its conventional form in [21]. Later in [22, 23, 24], the method of gas mixtures was introduced, where instead of pressurizing the intake manifold with air, a gas mixture was used. In the outlined publications, the mixture of gas was synthesized from air and argon at different proportions, corresponding to c_p/c_v of 1.40, 1.50, 1.60 and 1.67 at room temperature. This allows a gradual variation of the peak in-cylinder bulk gas temperature (thermal load), independent of the PCP (pressure load). The peak of the bulk gas temperature that can be achieved by this setup modification is around 1100°C.

For this motored configuration, the shunt pipe proved to be a very convenient modification to recycle the exhaust gas. A blow-by recirculation system was also adopted which collected the blow-by from the engine breathers and pressurised it back to the intake manifold. This means that the only gas escaping the system was that which could have leaked from the imperfections of the gasket faces between any two components. This quantity is however extremely small. A photo of the setup is shown in Figure 1.

For the purpose of in-cylinder heat transfer studies, the cylinder head combustion chamber surface was instrumented at two locations using surface thermocouples of the eroding type. One surface thermocouple was fitted in place of the OEM injector, and the other surface thermocouple was fitted at a custom-drilled location in the cylinder head, which coincides with the squish region at the periphery of the cylinder. The two instrumented locations on the cylinder head surface, and the corresponding piston locations on the piston are shown in Figure 2 and Figure 3 respectively.

FIGURE 1 The pressurised motored experimental setup.

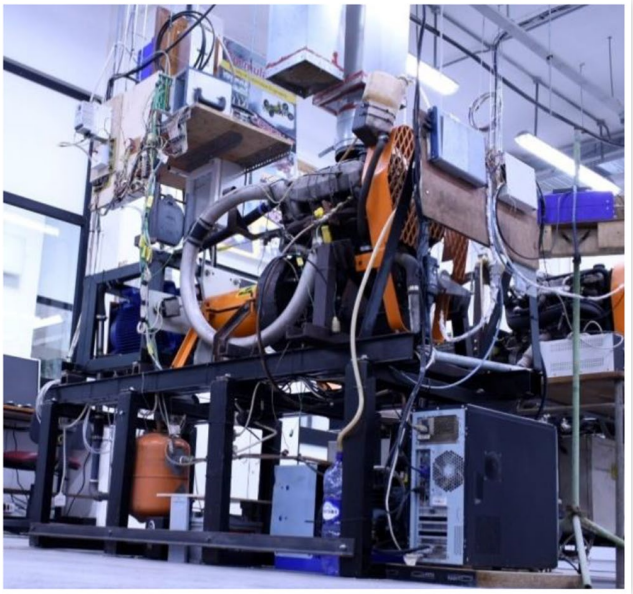

FIGURE 2 The instrumented locations on the cylinder head surface.

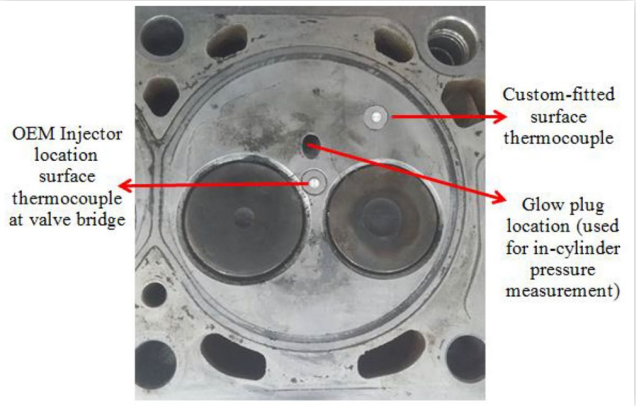

FIGURE 3 Locations on the piston crown that correspond to the cylinder head instrumented locations.

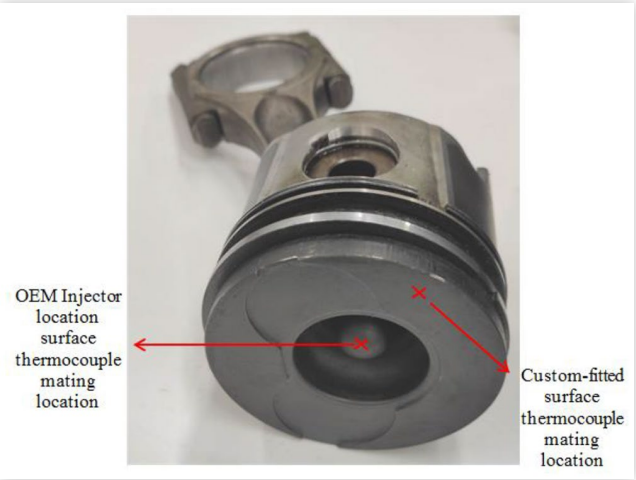

The cylinder head of the 2.0 HDi engine is made from aluminum. The adapters by which the surface thermocouples were fitted in the cylinder head were also made out of aluminum. For fitment of the surface thermocouples in the cylinder head, initially, interference fitment was seriously considered. However, from preliminary experiments it transpired that occasional thermocouple junction failure occurs, especially when testing at high bulk gas temperatures. As a result the thermocouples had to be fitted using an adapter for easier maintenance (re-establishment of junction). To avoid crevices originating in threads, the adapters were made to seal against the cylinder head using a copper washer. The thermocouple was secured to the adapter using a compression fitting. Any crevices in the adapter that were exposed to the bulk gas were purposely made with a tight sliding fit, to limit the crevice volumes as much as possible.

At the OEM injector location, a recessed thermocouple could not be fitted due to space restriction dictated by the cylinder head geometry. At the custom-drilled location, however, a recessed thermocouple was fitted, with the initial plan being to obtain the steady-state heat flux component from Fourier's law of one-dimensional conduction. Unfortunately, after conducting several preliminary tests, it transpired that significant errors were incurred on the steady-state heat flux component due to the sources outlined in the first part of this paper. As a result, data obtained from this recessed thermocouple was not used. The steady-state component of heat flux was instead obtained from a zero-dimensional calculation, based on the first law of thermodynamics on the closed part of the cycle, using the experimentally measured in-cylinder pressure. Whilst it is appreciated that this calculation can only give a global measurement, it is thought that with the present limitations in the experimental setup, it would be better to settle for a more modest and faithful result obtained through the first law, instead of the significantly error-biased measurement from the recessed thermocouple.

Finding the Transient Component of Heat Flux

The surface temperature swing as recorded by the surface thermocouple cannot be represented by a simple mathematical function. As a result, several authors [2, 4, 5, 6] in classical studies have converted the temperature signal into its equivalent frequency domain and represented as a finite series of sines and cosines, or cosines and phase angles. To be able to represent the surface temperature swing by a finite number of terms, the first N harmonics have to be chosen, out of a maximum equal to half of the number of ordinates in one complete cycle of the periodic signal. Making use of all the frequencies, in theory, gives the most accurate representation of the temperature signal, however if all harmonics are considered, noise interference captured in the thermocouple signal (and usually present at the higher end of the frequency spectrum) would result in disturbances in the heat flux signal. As a result, a number of harmonics is usually chosen that creates a good balance between having a properly represented temperature trace, whilst limiting the amount of disturbances originating from noise interference. Using too few of harmonics could lead to important phenomena in the temperature spectrum being unrepresented. Decreasing significantly the number of harmonics can also lead to the 'Gibbs Phenomenon'. Several authors who made use of this method had settled for around 70 harmonics [1, 7]. Once the temperature swing is properly represented, the temperature gradient at the heated surface could be found and applied in Fourier's law of one dimensional conduction. As a result, an inherent assumption that underlines the use of this method is that the heat flux at the surface of the thermocouple travels perpendicular to the heated surface. This assumption is often violated with the commercially available fast response thermometers, as explained in the first section of this paper. Another limitation that surrounds this method is that the Fourier's law of one-dimensional conduction permits only the input of thermo-physical properties of a single material through which heat assumingly flows.

The two limitations/inaccuracies highlighted for the method of spectral analysis can be somewhat reduced if the Impulse Response method is utilized in the conversion of the surface temperature swing to heat flux. The impulse response method was put forward by Oldfield [15] initially for turbine heat flux measurements, but was later applied to the engine heat flux problem by Buttsworth [10] and Wang [12].

The impulse response method makes use of a discrete deconvolution of a pair of known 'basis functions' of temperature and corresponding heat flux that characterize the behavior of the sensor by which engine experiments are conducted. The heat flux imposed can be a step function (which results in a monotonically increasing temperature). The resulting temperature from this known heat flux can be obtained in at least three ways; using an analytical solution, using a numerical solution, or from thermocouple characterization experiments that were presented in detail by [9, 12, 16]. Once the temperature response resulting from the known imposed heat flux is obtained for a given sampling frequency, a deconvolution algorithm between the imposed heat flux and obtained temperature is used to obtain an 'Impulse Response Function', *h(t)*. The impulse response function can then be convoluted with the temperature signal measured by the thermocouple in actual engine experiments to obtain the localised heat flux from the combustion chamber surface.

The Impulse Response method is applicable to any linear, time invariant system where the signal to be processed is initially steady. The response of any linear time invariant system can be obtained through the convolution integral given in equation (1), where q is the instantaneous heat flux, T is the instantaneous surface temperature, τ is a dummy variable and h is the impulse response function.

$$q(t) = h(t) * T(t) = \int_{-\infty}^{\infty} h(\tau)\, T(t-\tau)\, d\tau \qquad (1)$$

It is reported by Oldfield [15] that such integral can be difficult to evaluate in the time domain, and the impulse response function usually has singularities at the origin. In the discrete time domain, however, the surface temperature is sampled at a certain frequency and the convolution integral

can be written in the discrete convolution sum as in equation (2). In typical engine studies similar to that concerning this work, the sampling frequency is often related to the engine speed since the surface temperature signal acquisition is sampled according to an encoder coupled to the crankshaft. In this study, sampling was done at every $1/10^{th}$ of a crank angle degree.

$$q[n] = h[n] * T[n] = \sum_{k=0}^{N-1} h[k]T[n-k]$$

$$= \sum_{k=0}^{N-1} h[n-k]T[k] \qquad (2)$$

Apart from other advantages that the impulse response method offers which will be discussed at length later in the paper, this method also offers the advantage of not requiring the zero padding scheme and the windowing technique that are required by the Fourier spectral analysis method to ensure periodicity. This therefore makes the impulse response method slightly easier to implement. When employing the impulse response method, a sufficiently long surface temperature signal must be convoluted, instead of an ensemble average temperature. The reason for this is that the method will induce a starting transient on the computed heat flux which will eventually settle after a few cycles, hence the very first few cycles of computed heat flux needs to be discarded and the remaining heat flux cycles can then be ensembled to yield one representative heat flux cycle of the tested setpoint. To understand better this starting transient phenomena, a test was done in which a constructed 50 Hz sine wave with 32 identical cycles was used as the hypothetical sampled temperature signal. The resulting heat flux was obtained through the discrete convolution of this constructed temperature signal with the impulse response determined from the 1D semi-infinite solid solution assumption. The result consequently consisted of 32 heat flux cycles. In a separate run, a single 50 Hz sine wave temperature signal identical to that in the previous run was processed using the Fourier spectral analysis method. Figure 4 shows the heat fluxes of the first and last (32nd) cycles obtained from the impulse response method, and that obtained from the Fourier spectral analysis method. It can be seen that the last cycle from the impulse response method matches exactly that obtained from the Fourier spectral analysis method, however the first heat flux cycle from the impulse response method starts out distorted and settles later in the cycle. This demonstrates the starting transient induced by the impulse response. It was noticed that from the third cycle onwards, the heat flux settles almost completely and hence only very few starting cycles need to be discarded.

The surface temperature recorded from an internal combustion engine would naturally not start at zero temperature, but would be relatively steady throughout the majority of the intake and exhaust strokes, and hence for this matter, to employ the impulse response method, the recorded temperature signal has to be shifted by subtracting from it the initial temperature. The requirement of the Impulse Response method to process a long stream of data initially turns out to be slightly time consuming when obtaining the impulse response function. This process would escalate greatly in the time duration if the basis functions used for obtaining the impulse response function are obtained from numerical models or thermocouple characterization experiments, as explained in a forthcoming section. After obtaining the impulse response function, however, the method then becomes very computationally efficient since the obtained impulse response function can be convoluted with the sampled temperature over and over, as long as the thermocouple characteristics, the sampling frequency, or the sampled data length are unchanged.

FIGURE 4 The heat flux computed from the FFT method, the first cycle of the IR method, the 32nd cycle of the IR method and the constructed sine wave temperature.

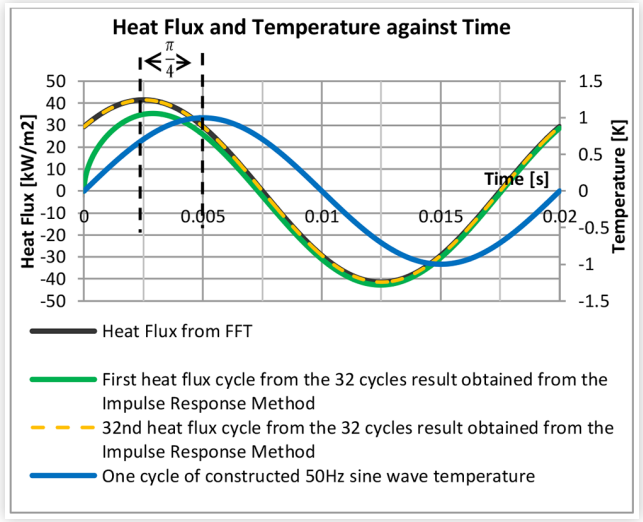

To reduce the computational time of the impulse response method the *decimate* function in Matlab was used to reduce the sample rate of the temperature signal by an integer factor of ten. This means that in the forthcoming section, the results obtained with the impulse response method were computed every one degree crank angle, as opposed to those computed from the Fourier spectral analysis method, which had a resolution of 1/10th of a crank angle degree.

One disadvantage underlying the impulse response method is the fact that the computed result is very sensitive to electrical noise interference in the sampled temperature signal. It is understood that this originates from the fact that the impulse response technique employs no filtering to the measured temperature signal. On the other hand, the more common Fourier spectral analysis method filters the electrical noise present at the high frequency components of the signal, when choosing the number of harmonics by which the temperature signal is represented. Hence, with the FFT method, the computed heat flux is less susceptible to disturbances originating from the sampled surface temperature. While this seems to be a disadvantage for the impulse response method, one can always employ a frequency filtering scheme on the sampled temperature and then use its result in the convolution integral of the impulse response method. This will however inherently decrease the simplicity of the impulse response method, as well as render its use more time consuming.

Accounting for Multi-Dimensional Heat Flux

The impulse response method has the characteristic that if the eroding thermocouple is well represented by the basis functions, then each evaluation of heat flux making use of the obtained impulse response function and sampled surface temperature will yield the heat flux at the surface of the sensor in line with the assumptions made in choosing the basis functions.

As explained in a previous section, the basis functions can be obtained from at least three methods; analytical models (usually assumed to be semi-infinite and one-dimensional), numerical models (which can be extended even up to three dimensions), or thermocouple characterization experiments. Using a one-dimensional analytical model is time efficient, and very low on computational effort. The one-dimensional analytical model is however known to be unable to well represent the actual heat flow phenomena at the surface of the fast response thermocouple. As a result, basis functions obtained from this method rank the lowest in terms of accuracy. Using numerical models is computationally expensive, but has the capability of offering a much more representative temperature response of the actual thermocouple in question. The best results in terms of accuracy can be obtained if the basis functions are obtained from thermocouple characterization experiments, which usually involve exposing the surface of the fast response thermocouple to a known heat flux originating from a focused laser beam, or shock wave experiments. This method gives the best results for the following reasons:

1. Variability induced in setting up the thermocouple junction is accounted for.
2. Thermal contact resistances between the different thermocouple materials are accounted for.
3. Thermo-physical properties of the materials involved in the thermocouple construction need not be determined from text books.

Even though thermocouple characterization experiments can provide the best results in terms of accuracy, it must be appreciated that conducting these experiments is time consuming, and not always possible in terms of apparatus required. Furthermore, if unaccounted for, latency of the thermocouple amplifier can bias the basis functions obtained, considering the very short rise time of the laser pulse (usually in nanoseconds) when compared to the surface temperature rise time of engine experiments (usually in a fraction of a millisecond).

In the study being put forward, the impulse response method was first employed making use of the basis function of temperature derived from the one-dimensional, semi-infinite solid assumption, and secondly through a two-dimensional finite element model. The imposed heat flux was a step of 1 MW/m^2 at the surface. The one-dimensional assumption was chosen initially so that the results obtained from the impulse response method could be checked against those obtained through the Fourier spectral analysis method. Recall that the Fourier spectral analysis method uses the same underlying assumption of a one-dimensional, semi-infinite solid conduction. The one-dimensional analytical model is described by equation (3), where $\sqrt{\rho ck}$ is the thermal product of the material through which all the one-dimensional heat flux assumingly flows (ρ: density, c: specific heat capacity, k: thermal conductivity), Q_o" is the applied step heat flux, T_1 is the resulting temperature and t is the time.

$$T_1(t) = \frac{2\,Q_o''}{\sqrt{\rho ck}}\sqrt{\frac{t}{\pi}} \qquad \ldots \qquad (3)$$

The numerical finite element, two-dimensional model, and results obtained from it are discussed in the next sub-section.

Two-Dimensional Finite Element Model

The finite element model conducted in this research was implemented using Ansys® Academic Research Mechanical, Release 2019 R3. The two-dimensional model consisted of a plane surface of unit thickness made up of four different materials; two of which are the thermocouple dissimilar materials (ANSI type E), and the others are the Mica insulator, and the split-tapered insert material. A transient thermal analysis was performed. Figure 5 shows the model set up, whilst Figure 6 shows a microscope image of the eroding thermocouple, indicating the modeled section on plane AA (note that the coordinate system is shown in both figures to illustrate the chosen analysis plane). An X-ray image of the eroding thermocouple is also given in Figure 7. From this figure, it was determined that the split-tapered inserts penetrate a distance of around 16.8 mm from the surface of the thermocouple.

For this research, three types of eroding thermocouples were procured; with aluminum split-tapered inserts, with stainless steel split-tapered inserts, and with zirconia split-tapered inserts. The stainless steel and zirconia thermocouples had a diameter of 1/8”, whereas the aluminum thermocouple had to be procured with a diameter of 1/4" due to manufacturing limitations. These different thermocouples were procured to investigate the differences in the surface temperature and heat flux reported by the three thermocouple types. Due to this, three variants of the finite element model had to

FIGURE 5 The finite element model. A: Constantan, B: Central Mica, C: Chromel, D E F G H: Split-tapered insert.

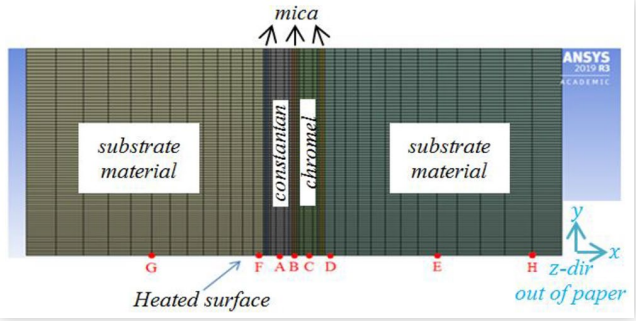

FIGURE 6 A microscope image of the exposed surface of the zirconia eroding thermocouple showing the modeled section on plane AA. The image shows the two thermocouple metals in a ribbon format and the two zirconia split-tapered inserts surrounded by the stainless steel tube.

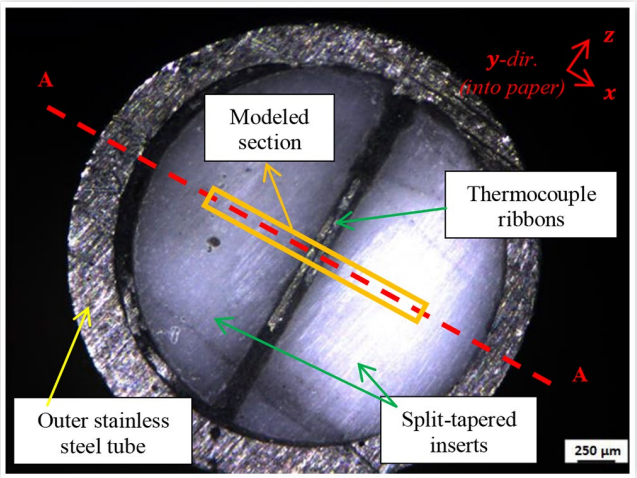

FIGURE 7 X-ray image of the eroding thermocouple, showing the thermocouple wires passing between the two split-tapered inserts, compressed by the outer stainless steel tube.

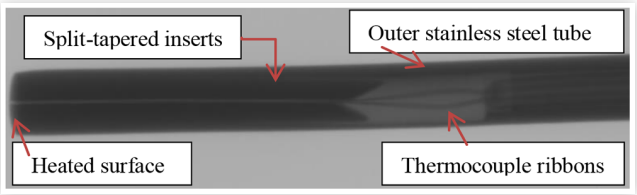

be constructed to represent the different split-tapered insert materials present in the three different thermocouples.

In engine experiments that were conducted in this research, the eroding thermocouples were used at engine speeds of 1400 rpm, 2000 rpm, 2500 rpm and 3000 rpm, hence the temperature data obtained through this testing campaign was sampled with four distinct sampling rates. The impulse response function obtained from the basis functions, and the sampled temperature needs to have the same amount of data points at the same sampling frequency. As a result, the finite element model was run with four distinct sampling rates, and heating times equivalent to the 300 consecutive engine cycles, similar to the experimentally acquired engine surface temperature measurements. This resulted in long simulation heating times of 25.7 seconds corresponding to 1400 rpm, down to 12 seconds for the engine speed of 3000 rpm. Since the *decimate* function was used with the impulse response method, the time step was equivalent to a 1 DegCA at the engine speed considered.

It was noted that for the very first few time increments of the finite-element analysis, numerical errors were resulting from a very steep initial increase in the temperature at the surface. Hence, for the first few time steps, a time step equivalent to 0.1 DegCA was imposed on the finite element model (instead of 1 DegCA).

The long heating times that the finite element model had to be run at resulted in the penetration of the heat flux deep in the axial direction (*y* direction) of the thermocouple. Since the model has a finite width (x-axis) and depth (y-axis) with thermally insulated boundary conditions, when the heating penetration in the *y* direction was sufficient, the insulated back face temperature of the model (extremity of y) increased from the initial value of 22°C and consequently resulted in a rapid increase in the heated face temperature, due to the reduced efficacy of heat diffusion. To prevent this, the length of the thermocouple model in the *y* direction was modeled to be the smallest possible such that the temperature gradient at the back insulated face remained zero throughout the duration of the simulation heating. According to a heat penetration calculation, for the longest heating time corresponding to that of 300 cycles at 1400 rpm, the axial lengths required for the zirconia, stainless steel and aluminum thermocouples were assigned to be 25 mm, 70 mm and 175 mm respectively. The different lengths of the 2D model required by the different sensors reflect the different thermal diffusivities of the three materials, with the aluminum having the highest diffusivity and the zirconia having the lowest diffusivity.

The issue of reduced heat diffusion efficacy just described also occurs if the temperature gradient in the *x* direction at the two insulated sides of the FEA model do not remain zero during the simulation heating time (due to two-dimensional heat flow). As a result, the modeled length in the *x* direction of the 2D split-tapered insert also had to be set to have sufficient length to allow undisturbed heat diffusion in the *x* direction. To avoid excessive computational times and large data files, while retaining a good mesh resolution, the thickness of the split-tapered material was limited to 0.25 mm for all the three sensors. This was expected to result in some deviation in the temperature response at the surface of the Central Mica and the other materials. To verify that this deviation was not excessive, the one-dimensional responses (for the longest heating time of 25.7 s - 300 cycles @ 1400 rpm) of the split-tapered inserts were plotted against the 2D temperature response of the split-tapered insert at the mesh node closest to the insulated side edge (point H in Figure 5). Any deviation of the 2D response at this point from the 1D response means that the heat conduction in the *x* direction is being suppressed by the side edge insulated boundary condition. It was noted that the deviation showed by the Aluminum thermocouple was equal to 4%, whereas that for the Stainless Steel thermocouple was equal to 1%. For the Zirconia thermocouple, a significant deviation of 25% was noted.

The thicknesses of the thermocouple dissimilar metals, and the mica sheets as designed in the finite element model were taken to be similar to those measured from the microscope images, *i.e.* the three mica sheets being 5 μm thick and the two thermocouple ribbons having a thickness of 25 μm.

The long lengths in the *y* direction assigned to the FEA models naturally resulted in a large number of elements, and hence a relatively long computational time. To decrease the computer processing as much as possible, the length of the materials in the *y* direction was discretized with a smoothly increasing element length starting with 1 μm at the heated

surface and increasing with length according to a bias factor, which was different for each FEA model, and dependent on the model length. The discretization of each material in the x-axis varied depending on the width of the different materials. The discretization was set to be fine at the material boundaries and coarse at the centre of each material. It was made sure that the mesh was as regular as possible, also ensuring that the aspect ratio is within acceptable limits. The finite element model was checked for convergence and mesh independence. The thermal resistance at the materials interface was set to be very small. This might be debatable, however it is noted that in the actual construction of the thermocouple, the split-tapered pins are forced into the tube and hence pressed considerably.

To aid in the understanding of the forthcoming results, Table 2 presents the thermophysical properties of the materials that make up the different eroding surface thermocouples. These values were also used in the finite element model.

Results from Finite Element Model

In this section, the results obtained from the finite element models corresponding to the three different thermocouples will be presented and discussed. Results of the temperature response obtained from the finite element models, and the corresponding imposed heat flux were eventually used as the basis functions in the impulse response method.

Figure 8, Figure 9 and Figure 10 show the temperature increase at the heated surface of the different materials making up the thermocouples, as obtained from the finite element model, in response to a step heat flux of 1 MW/m^2.

The temperature traces for the aluminum-based thermocouple given in Figure 8 show that the temperature response of the 2D central mica rises much more rapidly compared to the 2D temperature response of all other materials in the sensor. This is due to the much lower thermal conductivity of the mica compared to the other materials. It is shown that the

TABLE 2 Thermo-physical properties of the materials making up the eroding thermocouples used in this work.

	k [W/mK]	Density [kg/m^3]	Specific Heat Capacity [J/kgK]
*Zirconia	1.8	6090	427.0
**Mica	1.6	2800	56.5
‼Chromel	19.2	8730	448.0
‼Constantan	21.2	8920	393.6
†Aluminium	190.0	2800	896.0
††Stainless Steel	15.1	7750	480.0

*Ansys 2019 R3

**Buttsworth [10] and Wang [12]

‼Caldwell [25]

†Callister and Rethwisch [26]

††Ansys 2019 R3

FIGURE 8 The temperature response to 1 MW/m^2 step heat flux at the surface of the aluminum eroding thermocouple.

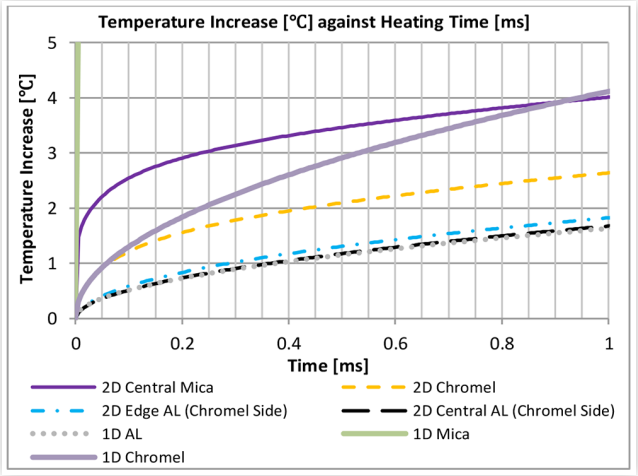

FIGURE 9 The temperature response to 1 MW/m^2 step heat flux at the surface of the stainless steel eroding thermocouple.

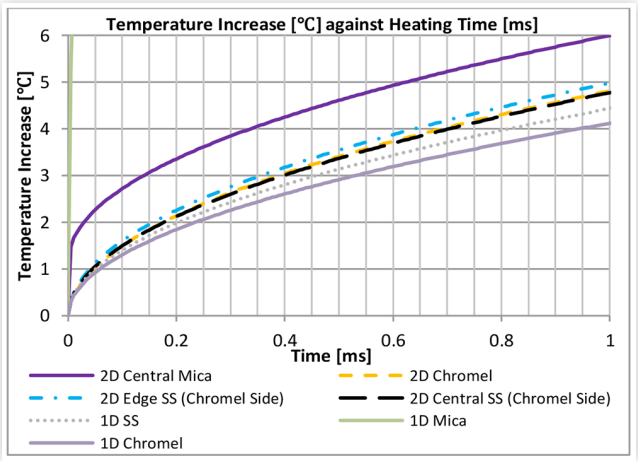

FIGURE 10 The temperature response to 1 MW/m^2 step heat flux at the surface of the zirconia eroding thermocouple.

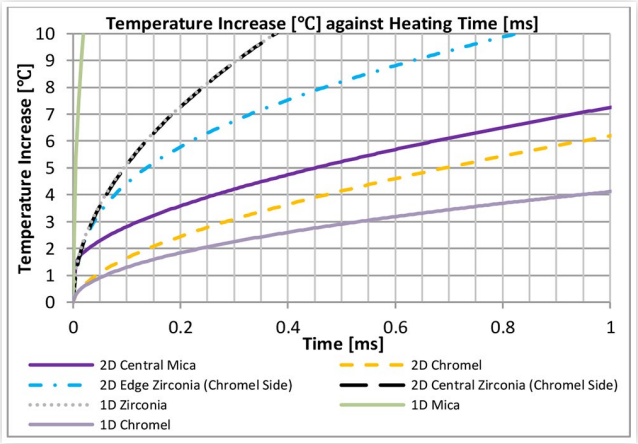

2D mica response is significantly different than the 1D mica response from a very early time. This is attributed to the heat flow in the *x* direction occurring from the Mica to the two thermocouple ribbons (chromel and constantan) due to the low diffusivity of the mica, which has a temperature above that of the metallic ribbons. The temperature response of the 2D chromel and 2D constantan also deviate from that of the 1D chromel at around 0.05 ms. This is due to the heat flow in the *x* direction from the two ribbons to the aluminum split tapered inserts, which act as a heat sink to the two thermocouple ribbons. As a result of this heat flow from the thermocouple ribbons to the aluminum, the temperature of the aluminum close to the Mica material (Edge AL) separating each thermocouple ribbon from the split-tapered insert increases slightly above that of the 1D Aluminum response. On the other hand, at a significant lateral distance from the mica edge, into the aluminum, the temperature of the aluminum (Central AL) is identical to that of the 1D aluminum response. It is interesting to note that both the temperature responses of the 2D Chromel and 2D Constantan are very similar. This is not shown in the figure due to clarity. The similar 2D temperature response of Chromel and Constantan is also reflected in the temperature responses of the 2D aluminum at the chromel and constantan sides, resulting in an almost thermally symmetric scenario, about the central Mica.

Figure 9 gives the temperature response of the Stainless Steel-based thermocouple. It is noted that the two-dimensional responses of the metallic elements in the thermocouple (stainless steel, chromel and constantan) are very similar. The only different temperature response is that originating from the central mica. This means that the high temperature retained at the central mica surface distributes heat to the surrounding thermocouple ribbons and consequently into the stainless steel split-tapered inserts. Due to this flow of heat in the *x* direction, the temperature response of the 2D mica is less than that expected from its 1D response. Consequently, the 2D response of the chromel element is higher than the 1D response of chromel. This also applies for constantan, even though its temperature response is not shown in the figure. Figure 9 also shows that the 2D temperature response of the stainless steel material, close to the side-mica interface is higher than that of the stainless steel away from the mica interface. This is understandable due to its proximity to mica. On the other hand, the temperature response of the stainless steel material away from the interface traces exactly the temperature response of the 1D stainless steel.

The temperature response of the zirconia-based sensor, given in Figure 10 shows the largest deviations between every different material making up the sensor. It is shown that after around 0.02 ms, the 2D zirconia away from the mica interface (central zirconia) obtains the highest temperature, which is identical to the 1D temperature response of zirconia. This means that after 0.02 ms, the zirconia material provides lateral heat conduction to the mica, and from the mica to the thermocouple ribbons. This is evidently shown by the fact that just below the 2D zirconia temperature response, one finds the temperature response of the zirconia at the mica interface (edge zirconia), then the central mica, and the lowest temperature is that of the thermocouple elements. The two-dimensional heat flow is very clearly shown by the fact that the 2D temperature response of chromel is much higher than what would be expected if one-dimensional conditions prevailed (shown by 1D chromel). Interestingly, below 0.005 ms, the central mica material seems to be at a higher temperature than the zirconia, but quickly cools off to the surrounding thermocouple elements. The rapid increase in the temperature of mica above that of the zirconia material results mainly from the very low specific heat capacity and low density of mica.

In the majority of the classical in-cylinder heat flux studies, researchers made use of the thermo-physical properties of the substrate material (split-tapered inserts) in the equation that describes the Fourier spectral analysis method of one-dimensional heat flux. It was well known, even in earlier times, that the thermo-physical properties of the split-tapered inserts material cannot fully describe the actual heat flux occurring at the surface of the thermocouple. For this reason, authors performed experiments on the thermocouples to try to determine a value of the thermal product which characterizes the composite thermocouple construction. While this method is somewhat more accurate than using the thermo-physical properties of just the split-tapered insert material, it was argued [18] that one value of the thermal product cannot describe the heat flux phenomena occurring at different timescales of interest. In simpler words this means that at short timescales the sensor material which dominates the axial heat flow is different than that which dominates at long timescales. This explanation is very clearly visible in the results given in Figure 8, Figure 9 and Figure 10. For the forthcoming discussion of the observation, let us assume that the actual thermocouple measures the surface temperature of the chromel or constantan (*i.e.* the junction is physically located on the chromel or constantan).

Figure 8 shows that after just 0.05 ms, the two-dimensional response of chromel deviate greatly from its one-dimensional analytical assumption. After 0.05 ms, the two-dimensional chromel response behaves similarly to that of aluminum, meaning that beyond this timescale, heat flux is mostly dominated by the aluminum material. A similar observation from Figure 9 shows that for the stainless steel based thermocouple, the two-dimensional response of chromel remains similar to the one-dimensional analytical solution up to just 0.02 ms. From this time onwards, the two-dimensional response follows that of stainless steel. From Figure 10, the two-dimensional response of chromel retains one-dimensional characteristic for 0.02 ms, but after this time duration closely follows the two-dimensional temperature response of the central mica, unlike the other two thermocouples. The observation made on chromel in this paragraph, is also similar to the behavior of constantan.

Having presented the two-dimensional temperature responses, it is clear that one set of thermo-physical properties cannot describe the heat flux phenomena occurring at different timescales. This observation highlights the importance of using a method that caters for multi-dimensional heat flow in the conversion from surface temperature measurement to heat flux.

In classical in-cylinder heat transfer research, [1, 19] to name a few, the base engine was made out of cast iron, and consequently the thermocouples used for surface temperature

measurements were also probably based on cast iron split-tapered inserts. The thermo-physical properties of cast iron lie somewhere between those of stainless steel, and aluminum; however closer to that of stainless steel. This means that while two-dimensional errors were surely incurred with the assumption of a one-dimensional heat flux, the extent of the error was probably much less than that which would be incurred in present studies if the same one-dimensional assumption is used. This is due to the fact that modern engines are normally based on either highly conductive materials such as aluminum, or highly insulative materials such as zirconia (for thermal barrier coatings). As have been shown in the presented figures, both aluminum and zirconia display a much worse two-dimensional effect, compared to the stainless steel thermocouple (and presumably cast iron).

To show the temperature gradients in the *x* direction set up in the respective materials for each of the three sensors, Figure 11 to Figure 13 give the surface temperature distributions at different heating times for the three sensors. In all these three figures, x = 0 correspond to the centre of the central mica. The boundary of the central mica - chromel is at 2.5 μm, the boundary of the chromel - side mica is at 27.5 μm, and the boundary of the side mica - split tapered insert is at 32.5 μm. As noted from these three figures, the temperature gradient at the insulated side of the thermocouple (*i.e.* approx.

FIGURE 11 Surface temperature distribution of the aluminum thermocouple.

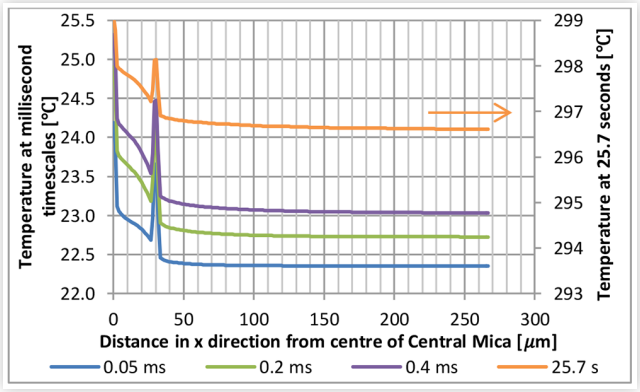

FIGURE 12 The surface temperature distribution of the stainless steel thermocouple.

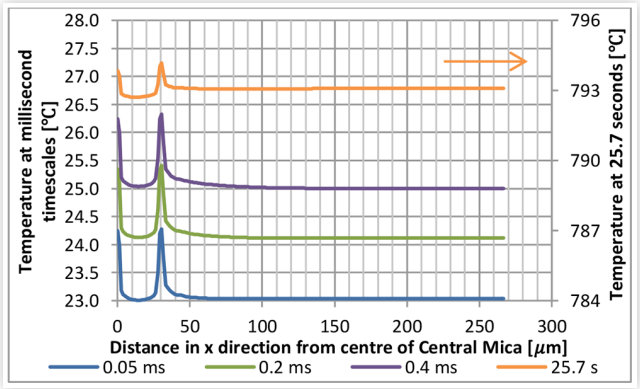

FIGURE 13 The surface temperature distribution of the zirconia thermocouple.

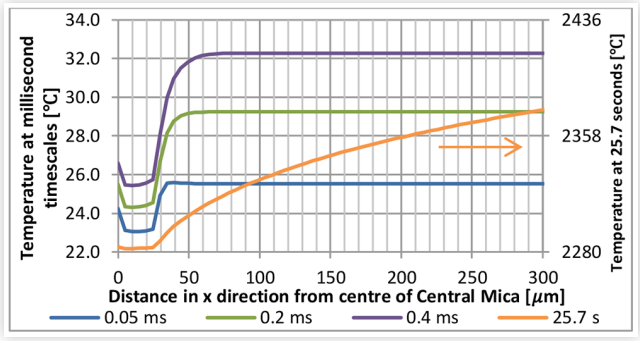

265 μm from the central axis) at the maximum heating time of 25.7 seconds is zero for both the stainless-steel and aluminum thermocouples. This shows that the thicknesses modeled in the finite element model for these two thermocouples were sufficient. On the other hand, for the zirconia thermocouple, it is shown that a significant temperature gradient was still evident at 300 μm away from the central axis for the same timescale of 25.7 seconds. Increasing the thickness of the zirconia split-tapered inserts to around 1 mm was found to be sufficient to decrease the temperature gradient in the *x* direction close to zero at the insulated side.

In the following section, the surface temperature and in-cylinder heat flux obtained from engine experiments are reported.

Engine Experiments

In the previous section, the effect of multi-dimensional heat flow through the eroding thermocouple was investigated in response to a step heat flux. In this section, results from engine experiments conducted on the pressurized motored setup are presented to demonstrate the error incurred in the heat flux measurement if multi-dimensional heat flux through the thermocouple is not accounted for. The surface temperature measurements and in-cylinder heat flux presented were obtained at the OEM injector location. Results from the custom-fitted location are not shown for conciseness. Figure 14, Figure 15 and Figure 16 show the surface temperature and transient component of in-cylinder heat flux recorded by the aluminum, stainless steel and zirconia thermocouples respectively. This data was obtained at 1400 rpm, 80 bar PCP and using air as the working gas. The surface temperature shown in these figures is an ensemble average over 300 cycles. It was noted that cycle-to-cycle variations were less than 0.5 °C throughout the entire 720° engine cycle. In all three figures, the in-cylinder heat flux is computed using both the Fourier spectral analysis method and the impulse response method. For the impulse response method, the basis functions were obtained from the one-dimensional analytical solution (using thermo-physical properties of the split-tapered inserts) and also from the two-dimensional finite element model, by assuming that the thermocouple junction lies on the chromel

FIGURE 14 Ensemble surface temperature measured by the aluminum thermocouple, and corresponding transient components of heat flux at 1400 rpm, 80 bar PCP, motoring.

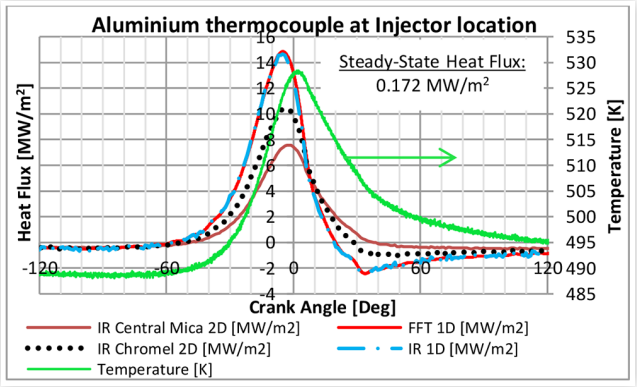

FIGURE 15 The ensemble surface temperature measured by the stainless steel thermocouple, and corresponding transient components of heat flux at 1400 rpm, 80 bar PCP, motoring.

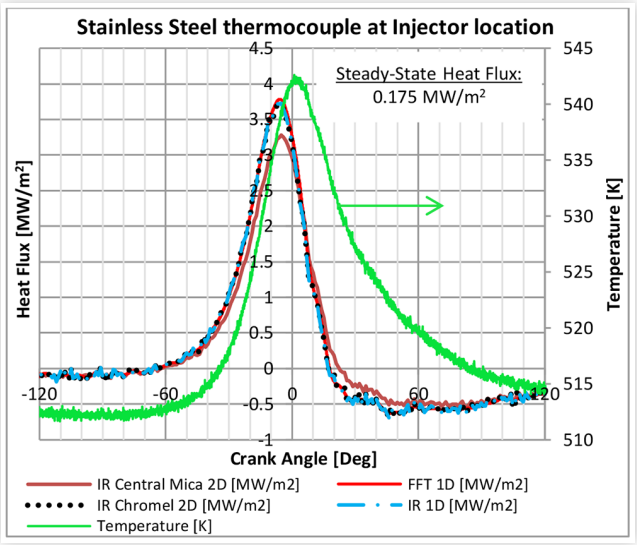

surface. The observations made on these three figures were also noticed for all other setpoints across the test matrix which ranged from engine speeds of 1400 rpm to 3000 rpm, PCPs of 80 bar and 100 bar, and working gases being air, argon and two gas mixtures in between.

FIGURE 16 The ensemble surface temperature measured by the zirconia thermocouple, and corresponding transient components of heat flux at 1400 rpm,80 bar PCP, motoring.

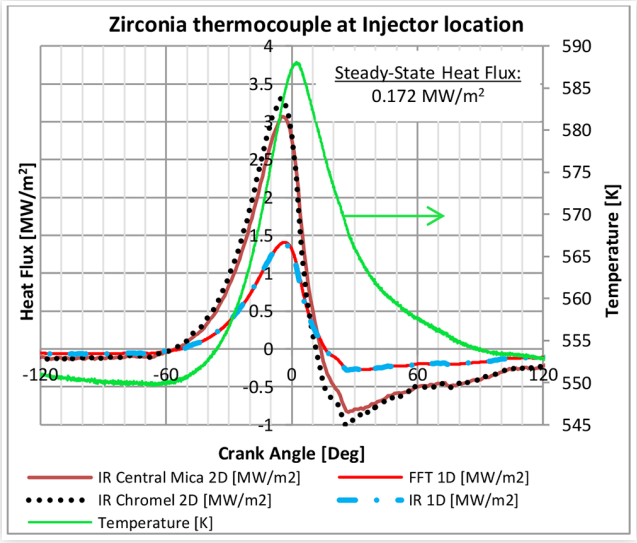

Through a comparative observation on the three figures, it is clearly visible that whilst the shape of the ensemble surface temperature seems common between the three different thermocouples, the mean value and the swing vary considerably. A summary of values obtained from Figure 14, Figure 15 and Figure 16 is given in Table 3 to facilitate interpretation. The aluminum thermocouple measures the lowest mean surface temperature, followed by the stainless steel and the zirconia thermocouples respectively. This is understandable and attributed to the high thermal diffusivity of aluminum. On the other hand, the swing of the surface temperature seems to be the lowest for the stainless steel thermocouple, whereas similar for both the aluminum and zirconia thermocouples. This observation was not totally understood. It was expected that for a similar heat flux, the aluminum should have shown the smallest surface temperature swing followed by stainless steel and zirconia. Out of the three different surface temperature swing measurements, the one measured by the aluminum seems to be the most unfitting. In fact, the transient component of heat flux obtained from the aluminum thermocouple resulted to be abnormally large when compared to that obtained from the stainless steel and zirconia thermocouples. Furthermore, the transient component of heat flux obtained from the stainless steel and zirconia thermocouples seem to

TABLE 3 Summary of values from Figure 14, Figure 15 and Figure 16.

	Minimum Surface Temperature [K]	Maximum Surface Temperature [K]	Temperature Swing [K]	Average Surface Temperature [K]
Aluminium Thermocouple	488	527	39	493.9
Stainless Steel Thermocouple	512	542	30	515.5
Zirconia Thermocouple	550	587	37	554.5

be in a similar order of magnitude to that reported by several researchers who also tested modern compression ignition engines in the pressurised motored state [2]. To ensure that the observation made by the aluminum thermocouple is not attributed to lack of setpoint reproducibility, the steady-state component of heat flux computed from the first law of thermodynamics on the closed part of the cycle, using measured in-cylinder pressure, is given in each of the three figures. It is noted that the difference between the three runs was low.

The aluminum thermocouple measurements given in Figure 14 will only be discussed with reference to multi-dimensional heat flux effects, but the reader has to remain cautious that this thermocouple reported anomalously high magnitudes of the transient component of heat flux. Figure 14 shows that the one-dimensional heat flux obtained using the Fourier spectral analysis method is identical to that obtained from the impulse response method when using basis functions from the one-dimensional analytical solution. This is expected since both methods are based on the same fundamental theory of a semi-infinite solid. When comparing the heat flux obtained through a one-dimensional consideration to that obtained through a two-dimensional consideration using the impulse response method, it is evident that the two-dimensional consideration shows significantly lower magnitudes. If one assumes the thermocouple to be measuring the central mica surface temperature, then the two-dimensional approach reports a heat flux which is half that reported by the one-dimensional consideration. The two-dimensional approach assuming the junction to be set up on the chromel surface shows a very similar heat flux to that obtained assuming that the junction is set up on the central mica. The latter however reports a slightly lower magnitude. The major discrepancy shown between one-dimensional and two-dimensional heat flux consideration is of concern, and highlights the importance of using computation methods that account for multi-dimensional effects in obtaining the transient component of heat flux from the cylinder of an internal combustion engine, something which in past researches might have been overlooked. This discrepancy in the heat flux magnitude between one-dimensional and multi-dimensional results can be understood as follows.

In the previous section, it was shown how the temperature simulated by the FEA model on the central mica in response to a step heat flux showed that for very early timesteps, the mica behaved in a one-dimensional manner, but after a very short time (on the order of 1 μs), the mica deviated away from the one-dimensional response and eventually started following the thermal behavior of the aluminum split-tapered inserts. If one considers this explanation when observing Figure 14, it becomes evident that during the short interval over which the surface temperature of the combustion chamber rises sharply, the temperature measured by the thermocouple on the central mica (or constantan/chromel ribbons) can be affected by the one-dimensional response of the mica. As a result, the sharp rise in heat flux reported by the 2D consideration will be less than that reported by a 1D consideration which assumes all heat flux to diffuse through aluminum (given the low thermal diffusivity of mica, compared to that of aluminum). On the other hand, when surface temperature fluctuation happens over a prolonged duration (say +60 DegCA to +180 DegCA - on the order of 10 ms), the temperature measured by the thermocouple on the central mica (or constantan/chromel ribbons) is highly characterized by the response of the aluminum. As a result, a 2D consideration will show very similar heat flux results when compared to a 1D consideration using thermo-physical properties of aluminum. The consideration of two-dimensional heat flux also showed a smaller negative magnitude and shifted to later crank angles when compared to the 1D consideration. In making this observation, the reader has to appreciate that the negative component of heat flux as reported in this figure is not absolute, given that the heat flux curve only shows the transient component. Had the steady-state component been added to the curves shown in this figure, all heat flux graphs would be shifted by the same quantity in the positive heat flux axis, meaning that the 2D heat flux would probably show no negative heat flux at all. A similar result to this was published previously by Wang [12] using a similar eroding thermocouple based on Dural, and also accounting for two-dimensional heat flux.

For the stainless steel thermocouple in Figure 15, the two-dimensional transient component of heat flux with the junction assumed to be on the central mica, shows lower magnitudes than the one-dimensional consideration. This can also be understood through the explanation given in the previous paragraph. For the stainless steel thermocouple, however, since the chromel and constantan ribbons have thermo-physical properties similar to those of the split-tapered stainless steel inserts, the two-dimensional effects are less severe.

The transient component of heat flux obtained from the zirconia thermocouple in Figure 16 shows that the one-dimensional heat flux assumption reports a magnitude which is half as that reported by the two-dimensional heat flux approach. This result also follows from the explanation given earlier which regards the timescale of the surface temperature rise and the consequent nature of heat flow of the different materials that make up the thermocouple. In this thermocouple, however, since the split-tapered inserts are made up of a material which has a very low thermal diffusivity, even at millisecond timescales the two-dimensional heat flux seems to still not retrace well the one-dimensional heat flux using the thermo-physical properties of zirconia. For a clearer understanding of this observation, the reader is referred to Figure 10 which shows that the temperature response of the two-dimensional central mica and chromel is significantly different than that of 1D zirconia, even at long timescales.

To better evaluate the comparison of the transient component of heat flux reported from the different thermocouples, Figure 17 shows the transient component of heat flux at 1400 rpm and 80 bar PCP as obtained from the stainless steel and zirconia thermocouple fitted at the OEM injector location, accounting for two-dimensional heat flux and assuming that the junction lies on the chromel surface. It is shown that throughout the cycle, the temporal variation, as well as the magnitude matches well, except for the negative part of the heat flux, which is faster for the zirconia thermocouple. On all other setpoints throughout the test matrix a similar match between the two thermocouples was found. As the engine speed increased, a better match was noted between the two

FIGURE 17 The transient component of heat flux at the OEM injector location at 1400 rpm and 80 bar PCP.

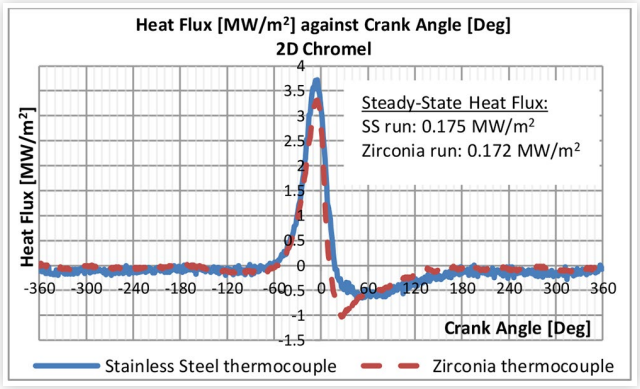

FIGURE 18 The transient component of heat flux at the OEM injector location at 3000 rpm and 80 bar PCP.

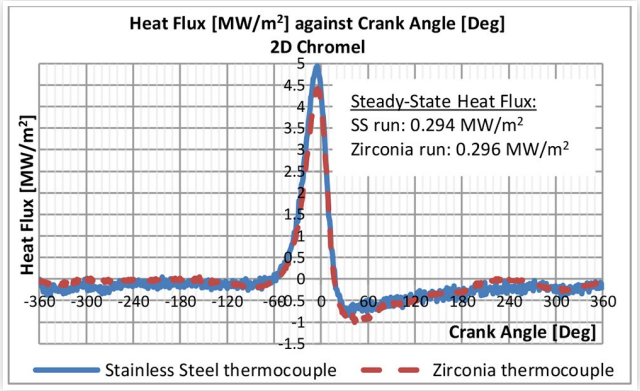

thermocouples throughout the cycle. Figure 18 shows the comparison at 3000 rpm, 80 bar PCP.

Conclusions

This research looked in detail at the problem of in-cylinder heat flux measurement through the use of three variants of the eroding-type surface thermocouple, fitted at two locations in the cylinder head of a 2.0 L pressurized motored engine. From this research it was appreciated that eroding surface thermocouples, and others of similar construction are complex instruments and their use requires care if robust heat flux data is to be obtained. This investigation concluded that the potential sources of errors in the experimental determination of the in-cylinder heat flux from surface thermocouple measurements originate from seven different (but related) shortcomings. Throughout this research, some of these shortcomings were addressed to the limit that practicality and reliability of the test engine allowed.

To cater for the most significant of the shortcomings presented, the Impulse Response method was used to account for the two-dimensional nature of heat flow through the surface thermocouples. This required results that were obtained from a two-dimensional finite element model that simulates the behavior of the heat flow through the thermocouple in response to a known step heat flux. Results showed that significant two-dimensional heat flow is evident with the zirconia and aluminum based thermocouples, but only a small degree of two-dimensional heat flux was noted with the stainless steel based thermocouple. Engine experiments showed that the error in the heat flux magnitude incurred when considering a one-dimensional heat flux consideration compared to a more realistic two-dimensional consideration were severe in the case of the aluminum and zirconia thermocouples, but small in the case of the stainless steel thermocouple. The phasing and magnitude of the negative portion of the heat flux were also found to vary between a one-dimensional and a two-dimensional heat flux treatment. It was also found that if two-dimensional heat flux is accounted for, the magnitude of the transient component of heat flux obtained from the zirconia and stainless steel thermocouples at the same experimental setpoint and fitted at the same location showed very similar shape and magnitude.

The above observations lead to two important conclusions:

1. The interested experimentalist should attempt to minimize as much as possible the seven sources of uncertainties highlighted in the first part of this publication. Of the mentioned uncertainties, the three most significant are the multi-dimensional heat flux through the thermocouple, the fitment of the thermocouple in the engine and ensuring the repeatability of the thermocouple rise time throughout the duration of the engine test.
2. The severity of multi-dimensional heat flux through the thermocouple, apart from other factors, is dependent on the thermocouple design, and hence cannot be eliminated. As a result, for a robust analysis, multi-dimensional heat flux must be accounted for in the post-processing of the temperature signal into heat flux. A three-dimensional model from thermocouple characterization experiments is ideal, however if this is not possible, a finite element model of the thermocouple that extends in two-dimensions is suggested instead of the more commonly used one-dimensional approach.

References

1. Overbye, V., Bennethum, J., Uyehara, O., and Myers, P., "Unsteady Heat Transfer in Engines," SAE Technical Paper 610041 (1961). https://doi.org/10.4271/610041.
2. Torregrosa, A.J., Bermúdez, V., Olmeda González, P.C., and Figueroa Garcia, O.L., "Experimental Assessment for Instantaneous Temperature and Heat Flux Measurements under Diesel Motored Engine Conditions," *Energy Conversion and Management* 54, no. 1 (2012): 57-66.
3. Hennes, C., Lehmann, J., and Koch, T., "Possibilities of Wall Heat Transfer Measurements at a Supercharged Euro VI Heavy-Duty Diesel Engine with High EGR-Rates, an In-

Cylinder Peak Pressure of 250 Bar and an Injection Pressure up to 2500 Bar," SAE Technical Paper 2019-24-0171 (2019). https://doi.org/10.4271/2019-24-0171.

4. Alkidas, A.C., "Heat Transfer Characteristics of a Spark-Ignition Engine," *Journal of Heat Transfer* 102 (1980): 189-193.
5. Hohenberg, G., "Advanced Approaches for Heat Transfer Calculations," SAE Technical Paper 790825, 1979, https://doi.org/10.4271/790825.
6. Alkidas, A.C., "Thermal Loading of the Cylinder Head of a Spark Ignition Engine," *Heat Transfer Engineering* 3, no. 3-4 (1982): 66-75, doi:10.1080/01457638108939585.
7. Farrugia, M., "Transient Surface Heat Flux Measurements in a Straight Pipe Extension of the Exhaust Port of a Spark Ignition Engine," PhD Dissertation, Oakland University, Rochester, Michigan, 2005.
8. Nanmac Corporation, "The Stem Effect," Leading Cause of Error in Temperature Measurement No. 92-2.
9. Gatowski, J.A., Smith, M.K., and Alkidas, A.C., "An Experimental Investigation of Surface Thermometry and Heat Flux," *Experimental Thermal and Fluid Science* 2 (1989): 280-292.
10. Buttsworth, D.R., "Transient Response of an Erodable Heat Flux Gauge using Finite Element Analysis," *Journal of Automobile Engineering* 216, no. Part D (2002): 701-706.
11. Buttsworth, D.R., Stevens, R., and Stone, C.R., "Eroding Ribbon Thermocouples: Impulse Response and Transient Heat Flux Analysis," *Measurement Science and Technology* 16, no. 7 (2005): 1487-1494, doi:10.1088/0957-0233/16/7/011.
12. Wang, X., Stone, R., Stevens, R., Arita, Y. et al., "Finite Element Analysis of Eroding Type Surface Thermocouple with Application to Engine Heat Flux Measurement," SAE Technical Paper 2006-01-1045 (2006). https://doi.org/10.4271/2006-01-1045.
13. Wendland, D.W., "The Effect of Periodic Pressure and Temperature Fluctuations on Unsteady Heat Transfer in a Closed System," NASA Report 72323, 1968.
14. Nijeweme, O.D., Kok, J.W., Stone, C.R., and Wyszynski, L., "Unsteady In-Cylinder Heat Transfer in a Spark Ignition Engine: Experiments and Modelling," *Journal of Automobile Engineering* 215, no. Part D (2001): 747-760.
15. Oldfield, M.L.G., "Impulse Response Processing of Transient Heat Transfer Gauge Signals," *Journal of Turbomachinery* 130, no. 2 (2008): 021023, doi:10.1115/1.2752188.
16. Bendersky, D., "A Special Thermocouple for Measuring Transient Temperatures," *Mechanical Engineering* (1953): 75.
17. Medtherm Corporation, "Bulletin 500," Huntsville, Alabama.
18. Buttsworth, D.R., "Assessment of Effective Thermal Product of Surface Junction Thermocouples on Millisecond and Microsecond Time Scales," *Experimental Thermal and Fluid Science* 25 (2001): 409-420.
19. Hoag, K., "Measurement and Analysis of the Effect of Wall Temperature on Instantaneous Heat Flux," SAE Technical Paper 860312 (1986). https://doi.org/10.4271/860312.
20. Caruana, C. and Farrugia, M., "Balancing of a Four Cylinder Engine for Single Cylinder Operation," in *19th Mechatronika IEEE Conference*, Prague, Czech Republic, 2020.
21. Caruana, C., Farrugia, M., and Sammut, G., "The Determination of Motored Engine Friction by Use of Pressurized 'Shunt' Pipe between Exhaust and Intake Manifolds," SAE Technical Paper 2018-01-0121, 2018, https://doi.org/10.4271/2018-01-0121.
22. Caruana, C., Farrugia, M., Sammut, G., and Pipitone, E., "Further Experimental Investigation of Motored Engine Friction Using Shunt Pipe Method," *SAE Int. J. Adv. & Curr. Prac. in Mobility* 1, no. 4 (2019): 1444-1453, https://doi.org/10.4271/2019-01-0930.
23. Caruana, C., Farrugia, M., Sammut, G., and Pipitone, E., "Experimental Investigation on the Use of Argon to Improve FMEP Determination through Motoring Method," SAE Technical Paper 2019-24-0141 (2019). https://doi.org/10.4271/2019-24-0141.
24. Caruana, C., Farrugia, M., Sammut, G., and Pipitone, E., "Further Experiments on the Effect of Bulk In-Cylinder Temperature in the Pressurized Motoring Setup Using Argon Mixtures," *SAE Int. J. Adv. & Curr. Prac. in Mobility* 2, no. 4 (2020): 2142-2155, https://doi.org/10.4271/2020-01-1063.
25. Caldwell, F.R., *Thermocouple Materials* (Washington: National Bureau of Standards, 1962)
26. Callister, W.D. and Rethwisch, D.G., "Appendix B: Properties of Selected Engineering Materials (Eight Edition)," in: , *Materials Science and Engineering: An Introduction*, (Wiley & Sons, 2010), A3-A30, ISBN:978-0-470-41997-7.

Contact Information

Mario Farrugia. Mechanical Engineering Department, University of Malta, Malta.
mario.a.farrugia@um.edu.mt

Carl Caruana. Mechanical Engineering Department, University of Malta, Malta.
carl.caruana.12@um.edu.mt

Acknowledgments

Prof. Martin Oldfield from Oxford University is thanked for his guidance in using the impulse response method, together with sharing his Matlab scripts.

The research work disclosed in this publication is partially funded by the Endeavour Scholarship Scheme (Malta). Scholarships are part-financed by the European Union-European Social Fund (ESF)-Operational Programme II-Cohesion Policy 2014-2020 "Investing in human capital to create more opportunities and promote the well-being of society".

Definitions/Abbreviations

AL - Aluminum

ATDC - After Top Dead Centre

BBDC - Before Bottom Dead Centre

BTDC - Before Top Dead Centre

CA - Crank Angle
CAD - Crank Angle Degrees
CARS - Coherent Anti-Stokes Raman Scattering
EVO - Exhaust Valve Opened
FEA - Finite Element Analysis
FFT - Fast Fourier Transform
HDi - High-Pressure Direct Injection
IR - Impulse Response
IVC - Intake Valve Closed
OEM - Original Equipment Manufacturer
OHC - Overhead Camshaft
PCP - Peak In-Cylinder Pressure
SI - Spark Ignition
SS - Stainless Steel

ISSN 0148-7191